1521-0111/12/8201-47–58
MOLECULAR PHARMACOLOGY
U.S. Government work not protected by U.S. copyright
Mol Pharmacol 82:47–58, 2012

Vol. 82, No. 1
76299/3775745

Neratinib Reverses ATP-Binding Cassette B1-Mediated Chemotherapeutic Drug Resistance In Vitro, In Vivo, and Ex Vivo[S]

Xiao-qin Zhao, Jing-dun Xie, Xing-gui Chen, Hong May Sim, Xu Zhang, Yong-ju Liang, Satyakam Singh, Tanaji T. Talele, Yueli Sun, Suresh V. Ambudkar, Zhe-Sheng Chen, and Li-wu Fu

State Key Laboratory of Oncology in South China, Cancer Center, Sun Yat-Sen University, Guangzhou, China (X.Z., J.X., X.C., X.Z., Y.L., L.F.); Laboratory of Cell Biology, Center for Cancer Research, National Cancer Institute, National Institutes of Health, Bethesda, Maryland (H.M.S., S.V.A.); and Department of Pharmaceutical Sciences, College of Pharmacy and Allied Health Professions, St. John's University, Jamaica, New York (S.S., T.T.T., Y.S., Z.S.C.)

Received October 10, 2011; accepted April 4, 2012

ABSTRACT

Neratinib, an irreversible inhibitor of epidermal growth factor receptor and human epidermal receptor 2, is in phase III clinical trials for patients with human epidermal receptor 2-positive, locally advanced or metastatic breast cancer. The objective of this study was to explore the ability of neratinib to reverse tumor multidrug resistance attributable to overexpression of ATP-binding cassette (ABC) transporters. Our results showed that neratinib remarkably enhanced the sensitivity of ABCB1-overexpressing cells to ABCB1 substrates. It is noteworthy that neratinib augmented the effect of chemotherapeutic agents in inhibiting the growth of ABCB1-overexpressing primary leukemia blasts and KBv200 cell xenografts in nude mice. Furthermore, neratinib increased doxorubicin accumulation in ABCB1-overexpressing cell lines and Rhodamine 123 accumulation in ABCB1-overexpressing cell lines and primary leukemia blasts. Neratinib stimulated the ATPase activity of ABCB1 at low concentrations but inhibited it at high concentrations. Likewise, neratinib inhibited the photolabeling of ABCB1 with [^{125}I]iodoarylazidoprazosin in a concentration-dependent manner (IC_{50} = 0.24 μM). Neither the expression of ABCB1 at the mRNA and protein levels nor the phosphorylation of Akt was affected by neratinib at reversal concentrations. Docking simulation results were consistent with the binding conformation of neratinib within the large cavity of the transmembrane region of ABCB1, which provides computational support for the cross-reactivity of tyrosine kinase inhibitors with human ABCB1. In conclusion, neratinib can reverse ABCB1-mediated multidrug resistance in vitro, ex vivo, and in vivo by inhibiting its transport function.

Introduction

Cancer cells may elude chemotherapy in a myriad of ways and share the ability to become resistant to numerous antineoplastic agents that are structurally and mechanistically unrelated. This trait, termed multidrug resistance (MDR), remains an impediment to effective chemotherapy of tumors (Gottesman et al., 2002). Diverse mechanisms contribute to the development of MDR, among which the most common reason is the overexpression of cell membrane-bound ATP-binding cassette (ABC) transporters. These transporters, at the expense of ATP hydrolysis, actively extrude diverse amphipathic chemotherapeutic agents, thus attenuating their cytotoxic effects and resulting in MDR (Dean et al., 2001; Pérez-Tomás, 2006). Forty-nine ABC transporters have been identified in the human genome and are divided into seven

This work was funded by the National Natural Sciences Foundation of China [Grants 81072669, 81061160] and the Natural Sciences Foundation of Guangdong Province [Grant 2008B030301331]. H.M.S. and S.V.A. were supported by the Intramural Research Program of the National Institutes of Health National Cancer Institute, Center for Cancer Research.

Article, publication date, and citation information can be found at http://molpharm.aspetjournals.org.

http://dx.doi.org/10.1124/mol.111.076299.

[S] The online version of this article (available at http://molpharm.aspetjournals.org) contains supplemental material.

ABBREVIATIONS: MDR, multidrug resistance; TKI, tyrosine kinase inhibitor; EGFR, epidermal growth factor receptor; Her-2, human epidermal receptor-2; ABC, ATP-binding cassette; P-gp, P-glycoprotein; DOX, doxorubicin; Rho123, Rhodamine 123; VRP, verapamil; PCR, polymerase chain reaction; PBS, phosphate-buffered saline; MTT, 3-(4,5-dimethylthiazol-2-yl)-2,5-diphenyltetrazolium bromide; PFS, progression-free survival; RT, reverse transcription; TBST, Tris-buffered saline/Tween 20; IAAP, iodoarylazidoprazosin; GAPDH, glyceraldehyde-3-phosphate dehydrogenase; PDB, Protein Data Bank; MK571, 3-[[[3-[(1*E*)-2-(7-chloro-2-quinolinyl)ethenyl]phenyl][[3-(dimethylamino)-3-oxopropyl]thio]methyl-]thio]propanoic acid.

subfamilies (termed A–G) on the basis of sequence similarities (Dean et al., 2001; Vasiliou et al., 2009), among which ABCB1 (P-glycoprotein, ABCB1/MDR1), ABCCs (multidrug resistance-associated proteins), and ABCG2 (breast cancer resistance protein/mitoxantrone resistance-associated transporter/ABCP) play major roles in producing MDR in tumor cells. These proteins share the ability to transport a large number of structurally diverse, mainly hydrophobic compounds out of cells; each transporter has its own unique substrates in addition to the overlapping substrate specificity (Szakács et al., 2006). Central to the mechanism of resistance to most chemotherapeutic regimens is the overexpression of ABCB1 protein, which extrudes (certainly but not only) *Vinca* alkaloids, anthracyclines, epipodophyllotoxins, and taxanes (Ambudkar et al., 1999).

It was reported that ABC transporters acted as modulators of oral absorption, and they have emerged as determinants of sanctuary sites (Shi et al., 2011). A number of blood-tissue barriers, including the blood-brain barrier, the maternal-fetal barrier, the blood-testicular barrier, and an apparent blood-cardiac muscle barrier, are mediated at least in part by ABC transporters (Sissung et al., 2011). In addition to their roles in protective barriers, ABC transporters decrease the penetration of antineoplastic agents into the targeted tissue compartments. Therefore, identification of agents that block ABC transporters at such sites, leading to increased drug penetration, would have potential clinical benefit well beyond a "reversal of MDR strategy" (Shi et al., 2011).

In particular, agents targeting EGFR and Her-2, such as lapatinib, have shown encouraging therapeutic efficacy (Wong et al., 2009). Neratinib is an orally available, irreversible, small-molecule, tyrosine kinase inhibitor of both EGFR and Her-2, acting at the ATP binding sites of their tyrosine kinase domains (Rabindran et al., 2004). Given the promising activity seen for neratinib, a large phase II trial examined the efficacy of neratinib among patients with Her-2-amplified breast cancer. The 16-week progression-free survival (PFS) rates were 59% for patients with previous trastuzumab treatment and 78% for patients with no previous trastuzumab treatment, and the median PFS times were 22.3 and 39.6 weeks, respectively (Burstein et al., 2010). Five of 35 patients exhibited partial responses with neratinib plus paclitaxel, whereas no dose-limiting toxicity was encountered in advanced Her-2-positive metastatic breast cancer in phase I/II trial NCT00445458 (http://clinicaltrials.gov). In phase I/II trial NCT00398567, patients with advanced Her-2-positive breast cancer that had progressed after trastuzumab therapy received 240 mg of neratinib with standard doses of trastuzumab. The overall response rate was 27%, which included 7% complete responses. The 16-week PFS rate was 45%, and the median PFS duration was 19 weeks. It is noteworthy that the findings of Seyhan et al. (2011) support a phase III clinical trial of neratinib with paclitaxel among patients with breast cancer. Three large phase III clinical trials using neratinib are currently ongoing. A phase III, randomized, open-label study (NCT00777101) comparing neratinib with a combination of capecitabine and lapatinib in locally advanced breast cancer or metastatic breast cancer with Her-2 amplification is ongoing. Neratinib is also being compared with placebo in a randomized double-blind phase III study (NCT00878709) of early-stage Her-2/Neu-overexpressing/amplified breast cancer after treatment with trastuzumab. Finally, a combination of neratinib plus paclitaxel is being compared with trastuzumab plus paclitaxel for the first-line treatment of Her-2-positive, locally advanced breast cancer or metastatic breast cancer (NCT00915018) (Alvarez, 2010). Therefore, neratinib will be the most-advanced drug in clinical study after lapatinib. Neratinib and trastuzumab exert their effects on the Her-2 receptor at different molecular sites, and it has been suggested that the combination of the two agents may be synergistic (Alvarez, 2010).

In our previous studies, we found that several tyrosine kinase inhibitors, including erlotinib (Shi et al., 2007), lapatinib (Dai et al., 2008), vandetanib (Zheng et al., 2009), cediranib (Tao et al., 2009), sunitinib (Dai et al., 2009), and apatinib (Mi et al., 2010), significantly attenuated or reversed ABC transporter-mediated MDR in cancer cells. Consequently, we conducted research to address whether neratinib could sensitize MDR cancer cells to conventional chemotherapeutic drugs and thus result in regression in a tumor xenograft model, through interaction with ABC transporters.

Materials and Methods

Reagents. Neratinib (HKI-272) was purchased from Wyeth-Ayerst (Princeton, NJ), with a molecular structure shown in Supplemental Fig. 1A. Monoclonal antibodies against ABCB1 and phosphorylated Akt (Ser473) were purchased from Santa Cruz Biotechnology, Inc. (Santa Cruz, CA). Akt antibody was obtained from Cell Signaling Technology, Inc. (Danvers, MA). The glyceraldehyde-3-phosphate dehydrogenase (GAPDH)-specific antibody was purchased from Kangchen Co. (Shanghai, China). Dulbecco's modified Eagle's medium and RPMI 1640 medium were products from Invitrogen (Carlsbad, CA). Platinum SYBR Green qPCR SuperMix-UDG with ROX was obtained from Invitrogen. Rhodamine 123 (Rho123), MTT, fumitremorgin C, paclitaxel, doxorubicin (DOX), vincristine, mitoxantrone, verapamil (VRP), 3-[[[3-[(1*E*)-2-(7-chloro-2-quinolinyl)ethenyl]phenyl][[3-(dimethylamino)-3-oxopropyl]thio]methyl]thio]propanoic acid (MK571; alternative name, L-660711), and other chemicals were purchased from Sigma-Aldrich (St. Louis, MO).

Cell Lines and Cell Culture. The following cell lines were cultured in Dulbecco's modified Eagle's medium or RPMI 1640 medium supplemented with 10% fetal bovine serum at 37°C in a humidified atmosphere of 5% CO_2: the human breast carcinoma cell line MCF-7, its DOX-selected, ABCB1-overexpressing derivative MCF-7/Adr (Fu et al., 2004), and the flavopiridol-resistant, ABCG2-overexpressing, MCF-7/FLV1000 subline (Robey et al., 2001), which was kindly provided by Dr. S. E. Bates (National Cancer Institute, National Institutes of Health, Bethesda, MD). The human oral epidermoid carcinoma cell line KB and its vincristine-selected, ABCB1-overexpressing derivative KBv200 were gifts from Dr. Xu-Yi Liu (Cancer Hospital of Beijing, Beijing, China). The human leukemia cell line HL60 and its DOX-selected, ABCC1-overexpressing derivative HL60/Adr and the human primary embryonic kidney cell line HEK293 and its stably pcDNA3.1- and ABCB1-transfected cell lines HEK293/pcDNA3.1 and HEK293/ABCB1 were obtained from Dr. S. E. Bates (National Cancer Institute). All of the transfected cells were cultured in medium with 2 mg/ml G418 (Geneticin) (Robey et al., 2003). All resistant cells were authenticated through comparison of their fold resistance with that of the parental, drug-sensitive cells and examination of the expression levels of ABC transporters. All cells were grown in drug-free culture medium for more than 2 weeks before assays.

Animals. Athymic nude mice (BALB/c-*nu/nu*), 5 to 6 weeks of age and weighing 18 to 24 g, were obtained from the Center of Experimental Animals, Sun Yat-Sen University (Guangzhou, China), and were used for the KBv200 cell xenografts. All animals received sterilized food and water. All experiments were performed in accor-

dance with the guidelines on animal care and experiments with laboratory animals (Center of Experimental Animals, Sun Yat-Sen University), which was approved by the ethics committee for animal experiments.

Patient Samples. Bone marrow samples from patients with acute myeloid leukemia that had been diagnosed according to the French-American-British classification were obtained with informed consent, and this study was approved by the ethics review committee at Sun Yat-Sen University. Leukemia blasts were isolated by using Ficoll-Hypaque density gradient centrifugation (GE Healthcare, Chalfont St. Giles, Buckinghamshire, UK), cultured in RPMI 1640 medium containing 10% fetal bovine serum, 100 U/ml penicillin, and 100 U/ml streptomycin, and incubated at 37°C in a humidified atmosphere containing 5% CO_2.

Cytotoxicity Assay. The MTT assay was performed as described previously, to estimate the sensitivity of cells to drugs (Chen et al., 2004b; Yan et al., 2008). In brief, cells were plated in 96-well microtiter plates and then various concentrations of neratinib and/or a full range of concentrations of conventional chemotherapeutic drugs were added to the wells. After 68 h of incubation, MTT (5 mg/ml, 20 μl/well) was added to the wells and the cells were incubated for an additional 4 h. The medium was then discarded, and 200 μl of dimethylsulfoxide was added to dissolve the formazan produced through the metabolism of MTT. The optical density was measured at 540 nm, with background subtraction at 655 nm, by using a model 550 microplate reader (Bio-Rad Laboratories, Hercules, CA). IC_{50} values were calculated from survival curves by using the Bliss method (Shi et al., 2006). The degree of resistance was estimated by dividing the IC_{50} for the MDR cells by that for the sensitive parental cells; the degree of reversal of MDR was calculated by dividing the IC_{50} values for the antineoplastic agents obtained in the absence of neratinib by those obtained in the presence of neratinib.

Nude Mouse Xenograft Model. The KBv200-inoculated nude mouse xenograft model established by Chen et al. (2004a) was used in this study. The xenograft model was found to maintain the MDR phenotype in vivo and was extremely resistant to paclitaxel treatment. In brief, KBv200 cells were harvested and implanted subcutaneously under the shoulder in the nude mice. When the tumors reached a mean diameter of 0.5 cm, the mice were divided randomly into four groups and were treated with the following regimens: 1) saline solution (every 3 days × four); 2) paclitaxel (18 mg/kg i.p., every 3 days × four); 3) neratinib (20 mg/kg p.o., every 3 days × four); and 4) paclitaxel (18 mg/kg i.p., every 3 days × four) plus neratinib (20 mg/kg p.o., every 3 days × four, administered 1 h before injection of paclitaxel). The body weights of the animals and the two perpendicular tumor diameters (A and B) were recorded every 3 days, and the tumor volume (V) was estimated according to the following formula (Chen et al., 2004a): $V = (\pi/6)[(A + B)/2]^3$.

The curves for tumor growth and body weight were drawn according to tumor volume and time of implantation. The mice were anesthetized and killed when the mean tumor weight in the control group was more than 1 g. Tumor tissues were excised from the mice, and their weights were measured. The ratio of growth inhibition (IR) was calculated according to the following formula (Chen et al., 2004a): IR = [1 − (mean tumor weight for experimental group/mean tumor weight for control group)] × 100%.

Flow Cytometry. Expression of ABCB1 in the primary leukemia blasts and the cell lines HEK293, HEK293/ABCB1, KB, and KBv200 was assessed through flow cytometry. Single-cell suspensions were prepared and washed three times with isotonic PBS (supplemented with 0.5% bovine serum albumin). Then, 10 μl of phycoerythrin-conjugated, mouse anti-human ABCB1 antibody was mixed with 25 μl of cells (4×10^6 cells per ml). After incubation for 45 min at 4°C in the dark, the cells were washed twice with PBS (supplemented with 0.5% bovine serum albumin) and were resuspended in 400 μl of PBS for flow cytometric analysis. Isotype control samples were treated in an identical manner with phycoerythrin-conjugated mouse IgG2α for ABCB1.

DOX and Rho123 Accumulation. The effects of neratinib on the accumulation of DOX and Rho123 in KB, KBv200, MCF-7, and MCF-7/Adr cells and of Rho123 in primary leukemia blasts were measured through flow cytometry, as described previously (Fu et al., 2004). The cells were treated for 3 h at 37°C with neratinib at various concentrations or vehicle. Then, 10 μM DOX or 5 μM Rho123 was added and incubation was continued for additional 3 or 0.5 h, respectively. The cells were collected, washed three times with ice-cold PBS, and analyzed through flow cytometry (Cytomics FC500; Beckman Coulter, Inc., Fullerton, CA). VRP, an ABCB1 inhibitor, was used as a positive control.

RT-PCR and Real-Time RT-PCR. ABCB1 expression was assayed as described previously (Dai et al., 2008). After treatment for 48 h, total cellular RNA was isolated with a TRIzol reagent RNA extraction kit (Molecular Research Center, Cincinnati, OH), by following the manufacturer's instructions. The first-strand cDNA was synthesized with oligo(dT) primers with reverse transcriptase (Promega, Madison, WI). The PCR primers were 5′-cccatcattgcaatagcagg-3′ (forward) and 5′-gttcaaacttctgctcctga-3′ (reverse) for ABCB1 and 5′-ctttggtatcgtggaagga-3′ (forward) and 5′-caccctgttgctgtagcc-3′ (reverse) for GAPDH. With the use of a GeneAmp 9700 PCR system (Applied Biosystems, Foster City, CA), reactions were performed at 94°C for 2 min for initial denaturation and then at 94°C for 30 s, 58°C for 30 s, and 72°C for 1 min. After 32 cycles of amplification, additional extension was performed at 72°C for 10 min. Products were resolved and examined through 1.5% agarose gel electrophoresis. Expected PCR products were 157 bp for ABCB1 and 475 bp for GAPDH.

Real-time RT-PCR was performed with a Bio-Rad CFX96 real-time system (Applied Biosystems). The geometric mean of GAPDH levels was used as an internal control, to normalize the variability in expression levels. The forward primer for GAPDH was 5′-gagtcaacggatttggtcgt-3′, and the reverse primer was 5′-gatctcgctcctggaagatg-3′. The forward primer for ABCB1 was 5′-gtggggcaagtcagttcatt-3′, and the reverse primer was 5′-tcttcacctccaggctcagt-3′. PCR was performed at 50°C for 2 min, at 95°C for 5 min, and then at 95°C for 15 s and 60°C for 30 s for 40 cycles. Relative quantification of ABCB1 was performed by using the threshold cycle difference method (Livak and Schmittgen, 2001). To ensure reproducibility of the results, all genes were tested in triplicate in three independent experiments.

ABCB1 ATPase Activity Assay. Verapamil-stimulated ABCB1 ATPase activity was estimated with a Pgp-Glo assay system (Promega). The inhibitory effect of neratinib was examined against verapamil-stimulated ABCB1 ATPase activity. Sodium orthovanadate (Na_3VO_4) was used as an ABCB1 ATPase inhibitor. Neratinib at various concentrations, diluted with assay buffer, was incubated with 0.1 mM VRP, 5 mM MgATP, and 25 μg of recombinant human ABCB1 membranes at 37°C for 40 min. Subsequently, luminescence was initiated with ATP detection buffer. After incubation at room temperature for 20 min, to allow the luminescent signal to develop, the untreated, white, opaque, 96-well plate (Corning Life Sciences, Lowell, MA) was read with a luminometer (SpectraMax M5; Molecular Devices, Sunnyvale, CA). The changes in relative light units were determined by comparing Na_3VO_4-treated samples with neratinib/VRP combination-treated samples, and the ATP consumed was measured through comparison with a standard curve.

Laser Scanning Confocal Microscopy. Coverslips (13 × 13 mm) were placed in the wells of a 24-well plate, and 2×10^4 cells were subcultured into a 24-well plate. After treatment, cells were fixed for 20 min with PBS containing 4% paraformaldehyde and were permeabilized for 10 min at room temperature with 0.25% Triton X-100 in PBS. After being washed three times with PBS, coverslips were treated for 1 h with blocking buffer (PBS with 0.1% Tween and 1% bovine serum albumin). For immunolabeling experiments, cells were incubated with Mdr-1 antibody (1:50; Santa Cruz Biotechnology, Inc.), washed, and incubated with Alexa Fluor 594 goat anti-mouse IgG (1:1000; Invitrogen). Nuclei were observed by using 4,6-diamidine-2-phenylindole (1:2000; Sigma-Aldrich). Cells were

observed through confocal microscopy (objective, 100×; FV1000; Olympus, Tokyo, Japan).

Photoaffinity Labeling of ABCB1 with [^{125}I]Iodoarylazidoprazosin. Photoaffinity labeling of ABCB1 with [^{125}I]iodoarylazidoprazosin ([^{125}I]IAAP) was performed as described previously (Sauna and Ambudkar, 2000). Insect cell crude membranes (500 μg/ml) were incubated with increasing concentrations (0–5 μM) of neratinib for 3 min at room temperature in 50 mM Tris-HCl, pH 7.5, after which 4 to 6 nM [^{125}I]IAAP (2200 Ci/mmol; PerkinElmer Life and Analytical Sciences, Waltham, MA) was added in subdued light. The samples were then exposed to ultraviolet light (365 nm) for 10 min at room temperature and were resolved on 7% Tris-acetate gels. The radioactivity in the ABCB1 band was quantified by using a Storm 860 molecular imaging system (GE Healthcare) and ImageQuaNT software (GE Healthcare).

Western Blot Analysis. To identify whether neratinib affects the expression of ABCB1, cells were incubated with various concentrations of neratinib for 48 h and with 1 μM neratinib for different periods of time. To determine whether neratinib is able to block Akt phosphorylation, the cells were incubated with different concentrations of neratinib for 24 h and with 1 μM neratinib for various periods of time. Whole cells were then harvested and washed twice with ice-cold PBS. Cell extracts were collected in cell lysis buffer (1× PBS, 1% NP-40, 0.5% sodium deoxycholate, 0.1% sodium dodecyl sulfate, 100 μg/ml phenylmethylsulfonyl fluoride, 10 μg/ml aprotinin, 10 μg/ml leupeptin) (Yan et al., 2011). Protein concentrations were quantified as described by Bradford (1976). Equal amounts of cell lysates from various treatments were resolved with sodium dodecyl sulfate-polyacrylamide gel electrophoresis. After blocking for 2 h at room temperature in TBST (10 mM Tris-HCl, 150 mM NaCl, 0.1% Tween 20, pH 8.0) with 5% nonfat milk, the membranes were incubated overnight at 4°C with appropriately diluted primary antibodies. The membranes were then washed three times with TBST and incubated for 2 h at room temperature with horseradish peroxidase-conjugated secondary antibody (1:5000 dilution). After three washes with TBST, the protein-antibody complexes were observed with an enhanced Phototope TM-HRP detection kit (Cell Signaling Technology, Danvers, MA) and were exposed to a Kodak medical X-ray processor (Carestream Health, Rochester, NY). GAPDH was used as a loading control.

Ligand Structure Preparation. Neratinib was built by using the fragment dictionary of Maestro 9.0 and was energy-minimized with Macromodel 9.7 (Schrödinger, Inc., New York, NY), by using the Optimized Potentials for Liquid Simulations-all atom force field with the steepest descent followed by the truncated Newton conjugate gradient protocol. The low-energy three-dimensional structures of neratinib were generated with the following parameters present in LigPrep 2.3 (Schrodinger, Inc., New York, NY): different protonation states at physiological pH, all possible tautomers, and ring conformations. The output obtained from the LigPrep analysis was used to generate 100 ligand conformations by using default parameters for the conformational search panel of the Macromodel submenu that uses a combination of mixed-torsional and low-mode sampling. Minimized structures were filtered with a maximal relative energy difference of 5 kcal/mol, to exclude redundant conformers. The output conformational search file containing 100 unique conformers of neratinib was used as input for docking simulations.

Protein Structure Preparation. The X-ray crystal structures of mouse ABCB1 in complexes with inhibitors QZ59-*RRR* (PDB no. 3G6O) for site 1 and QZ59-*SSS* (PDB no. 3G61) for site 2 and in an apoprotein state (PDB no. 3G5U) for sites 3 and 4 (Aller et al., 2009), obtained from the Research Collaboratory for Structural Bioinformatics Protein Data Bank (http://www.rcsb.org), were used as the templates to generate homology models for human ABCB1 for sites 1 to 4 (Shi et al., 2011). For evaluation of the possibility of neratinib interacting at the ATP binding site, the crystal structure of the LmrA-ATP binding domain from *Lactococcus lactis* (PDB no. 1MV5) (unpublished data), which includes 243 C-terminal residues (residues 342–583), was used as a template to generate the ATP-bound human ABCB1 homology model. The protocol for the homology modeling was essentially the same as reported previously (Shi et al., 2011). The refined human ABCB1 homology model was used to generate different receptor grids for different sites (sites 1–4) through selection of bound QZ59-*RRR* (site 1) and QZ59-*SSS* (site 2) ligands, all amino acid residues known to contribute to verapamil binding (site 3), two residues (Phe728 and Val982) known to be common to three previously determined sites (site 4), and bound ATP for the ATP binding site, essentially as reported previously (Shi et al., 2011). Moreover, the X-ray covalent complex of the EGFR kinase domain and neratinib (PDB no. 2JIV) (Yun et al., 2008) was energy-minimized according to the protein preparation tool present in Maestro and was used to compare the topological features of the ATP binding site of the kinase domain of EGFR with the topological features of the drug/substrate binding pocket of ABCB1, through residue charge surface representation.

Docking Protocol. The conformational library of neratinib was docked at each of the generated grids (sites 1–4 and the ATP binding site of ABCB1) by using the XP mode of Glide 5.0 (Schrödinger, Inc.) and the default parameters. The top-scoring pose-ABCB1 complex was then subjected to energy minimization by using Macromodel 9.7, with the Optimized Potentials for Liquid Simulations-all atom force field, and was used for graphical analysis. All computations were performed with a Dell Precision 470n dual-processor computer (Dell, Round Rock, TX) with the Linux operating system (WS 4.0; Red Hat Inc., Raleigh, NC).

Statistical Analyses. All experiments were repeated at least three times, and differences were determined by using Student's *t* test. Significance was determined at $P < 0.05$.

Results

Neratinib Reverses MDR in Cells Overexpressing ABCB1. The cytotoxicity of neratinib in different cell lines was determined with the MTT assay. The IC_{50} values were 4.13 ± 0.47, 6.03 ± 0.64, 3.30 ± 0.41, 2.88 ± 0.30, 3.02 ± 0.34, 7.09 ± 0.71, 2.26 ± 0.23, 1.42 ± 0.15, 5.29 ± 0.53, and 6.91 ± 0.70 μM for KB, KBv200, MCF-7, MCF-7/Adr, MCF-7, MCF-7/FLV1000, HL60, HL60/Adr, HEK293/pcDNA3.1, and HEK293/ABCB1 cells, respectively (Supplemental Fig. 1, B–F). On the basis of the cytotoxicity curves, more than 85% of cells were viable with neratinib at concentrations up to 1.0 μM in KB, KBv200, MCF-7, MCF-7/Adr, HEK293/pcDNA3.1, and HEK293/ABCB1 cells and 0.5 μM in HL60 and HL60/Adr cells. Therefore, neratinib concentrations of 1.0 μM (KB, KBv200, MCF-7, MCF-7/Adr, MCF-7, MCF-7/FLV1000, HEK293/pcDNA3.1, and HEK293/ABCB1 cells) or 0.5 μM (HL60 and HL60/Adr cells) were chosen as the maximal concentrations for combination treatment with ABCB1 (DOX, vincristine, and paclitaxel), ABCC1 (DOX), or ABCG2 (mitoxantrone) substrate anticancer drugs.

IC_{50} values for the antineoplastic drugs in sensitive and resistant cells with different concentrations of neratinib are shown in Table 1. Neratinib produced a concentration-dependent decrease in the IC_{50} values for DOX and vincristine in KBv200 cells and DOX in MCF-7/Adr cells. In contrast, neratinib produced only ~2-fold sensitization to DOX in the parental KB and MCF-7 cells. At the lowest concentration tested (0.25 μM), neratinib was still able to reverse resistance to DOX by 3.34- and 4.84-fold in KBv200 and MCF-7/Adr cells, respectively. Accordingly, 1 μM neratinib significantly decreased the IC_{50} values for DOX in stably transfected HEK293/ABCB1 cells (Table 2). There was no significant difference in the IC_{50} values for DOX in the pres-

TABLE 1

Effects of neratinib in reversing ABCB1-, ABCG2-, and ABCC1-mediated drug resistance

Cell survival rates were determined with MTT assays, as described under *Materials and Methods*. Data are the mean ± S.D. of at least three independent experiments performed in triplicate. The fold reversal of MDR was calculated by dividing the IC_{50} for cells with the anticancer agent in the absence of neratinib, VRP, or fumitremorgin C by that in the presence of neratinib, VRP, or fumitremorgin C.

Compounds	IC_{50} (Reversal)						
	KB	KBv200 (ABCB1)	MCF-7	MCF-7Adr (ABCB1)	MCF-7/FLV1000 (ABCG2)	HL60	HL60/Adr (ABCC1)
				μM (fold)			
Doxorubicin	0.031 ± 0.006 (1.00)	7.122 ± 0.430 (1.00)					
+ 0.25 μM Neratinib	0.025 ± 0.004 (1.26)	2.135 ± 0.103 (3.34)*					
+ 0.5 μM Neratinib	0.018 ± 0.003 (1.69)*	1.550 ± 0.278 (4.60)**					
+ 1.0 μM Neratinib	0.014 ± 0.003 (2.20)*	0.588 ± 0.207 (12.11)**					
+ 10 μM Verapamil	0.029 ± 0.004 (0.94)	0.250 ± 0.070 (28.45)**					
Vincristine	0.0025 ± 0.0002 (1.00)	1.440 ± 0.130 (1.00)					
+ 0.25 μM Neratinib	0.0025 ± 0.0004 (1.00)	0.765 ± 0.070 (1.88)**					
+ 0.5 μM Neratinib	0.0025 ± 0.0003 (1.00)	0.269 ± 0.028 (5.36)**					
+ 1.0 μM Neratinib	0.0021 ± 0.0003 (1.16)	0.035 ± 0.002 (41.17)**					
+ 10 μM Verapamil	0.0023 ± 0.0004 (1.06)	0.018 ± 0.001 (82.48)**					
Paclitaxel	0.0016 ± 0.0002 (1.00)	0.222 ± 0.021 (1.00)					
+ 0.25 μM Neratinib	0.0016 ± 0.0002 (1.00)	0.074 ± 0.009 (2.99)**					
+ 0.5 μM Neratinib	0.0015 ± 0.0001 (1.07)	0.022 ± 0.004 (10.13)**					
+ 1.0 μM Neratinib	0.0017 ± 0.0002 (0.94)	0.005 ± 0.001 (43.34)**					
+ 10 μM Verapamil	0.0016 ± 0.0003 (1.00)	0.004 ± 0.001 (50.76)**					
Cisplatin	3.022 ± 0.30 (1.00)	3.951 ± 0.40 (1.00)					
+ 1.0 μM Neratinib	2.888 ± 0.28 (1.05)	3.354 ± 0.34 (0.97)					
+ 10 μM Verapamil	2.943 ± 0.30 (1.03)	4.071 ± 0.40 (1.18)					
Doxorubicin			0.283 ± 0.02 (1.00)	11.675 ± 1.186 (1.00)			
+ 0.25 μM Neratinib			0.262 ± 0.03 (1.08)	2.413 ± 0.196 (4.84)**			
+ 0.5 μM Neratinib			0.215 ± 0.02 (1.31)*	1.443 ± 0.27 (8.09)**			
+ 1.0 μM Neratinib			0.163 ± 0.01 (1.74)*	0.944 ± 0.06 (12.37)**			
+ 10 μM Verapamil			0.285 ± 0.03 (0.99)	0.478 ± 0.076 (24.40)**			
Mitoxantrone			0.115 ± 0.012 (1.00)		6.723 ± 0.632 (1.00)		
+ 0.125 μM Neratinib			0.109 ± 0.011 (1.05)		6.231 ± 0.611 (1.07)		
+ 0.25 μM Neratinib			0.107 ± 0.011 (1.07)		6.081 ± 0.602 (1.11)		
+ 0.5 μM Neratinib			0.114 ± 0.010 (1.02)		5.149 ± 0.521 (1.31)		
+ 2.5 μM Fumitremorgin C			0.109 ± 0.011 (1.06)		0.276 ± 0.021 (24.36)**		
Doxorubicin						0.074 ± 0.007 (1.00)	3.622 ± 0.313 (1.00)
+ 0.125 μM Neratinib						0.078 ± 0.008 (0.95)	3.668 ± 0.367 (1.12)
+ 0.25 μM Neratinib						0.069 ± 0.006 (1.08)	3.600 ± 0.360 (1.14)
+ 0.5 μM Neratinib						0.061 ± 0.006 (1.21)	3.083 ± 0.301 (1.18)
+ 40 μM MK571						0.065 ± 0.006 (1.13)	0.0825 ± 0.008 (5.50)**

* $P < 0.05$ versus the values obtained in the absence of neratinib, VRP, or fumitremorgin C.
** $P < 0.01$ versus the values obtained in the absence of neratinib, VRP, or fumitremorgin C.

TABLE 2
Effects of neratinib in reversing ABCB1-mediated MDR in transfected cell lines

Cell survival rates were determined with MTT assays, as described under *Materials and Methods*. Data are the mean ± S.D. of at least three independent experiments performed in triplicate. The fold reversal of MDR was calculated by dividing the IC_{50} for cells with the anticancer drug in the absence of inhibitor by that in the presence of inhibitor.

Compounds	IC_{50} (Reversal)	
	HEK293/pcDNA3.1	HEK293/ABCB1
	μM (fold)	
Doxorubicin	0.074 ± 0.006 (1.00)	1.339 ± 0.130 (1.00)
+ 0.25 μM Neratinib	0.065 ± 0.006 (1.13)	0.756 ± 0.070 (1.77)**
+ 0.5 μM Neratinib	0.079 ± 0.008 (0.94)	0.332 ± 0.027 (4.03)**
+ 1.0 μM Neratinib	0.082 ± 0.007 (0.90)	0.167 ± 0.010 (7.98)**
+ 10 μM Verapamil	0.083 ± 0.008 (0.89)	0.094 ± 0.008 (14.19)**
Cisplatin	2.431 ± 0.27 (1.00)	2.681 ± 0.27 (1.00)
+ 1.0 μM Neratinib	2.263 ± 0.22 (1.07)	2.176 ± 0.22 (1.23)
+ 10 μM Verapamil	2.356 ± 0.23 (1.03)	2.344 ± 0.23 (1.14)

** $P < 0.01$ versus the values obtained in the absence of inhibitor.

ence or absence of neratinib in HEK293/pcDNA3.1 cells (Table 2). Neratinib did not significantly alter the IC_{50} values for cisplatin, a nonsubstrate of ABCB1, in any of the cell lines (Tables 1 and 2). Neratinib had no significant reversal effect on ABCC1-mediated drug resistance in HL60/Adr cells or ABCG2-mediated drug resistance in MCF-7/FLV1000 cells. These results suggest that neratinib significantly sensitizes ABCB1-overexpressing cells to antineoplastic agents that are substrates of ABCB1.

Neratinib Reverses ABCB1-Mediated MDR in the Nude Mouse Xenograft Model. An established KBv200 cell xenograft model in nude mice was used to evaluate the efficacy of neratinib to reverse resistance to paclitaxel in vivo. There was no significant difference in tumor size between animals treated with saline, neratinib, or paclitaxel, which indicates in vivo resistance to paclitaxel. However, the combination of neratinib and paclitaxel produced a significant inhibition of tumor growth, compared with saline, paclitaxel, or neratinib alone ($P < 0.05$) (Fig. 1, A and B). The tumor growth inhibition with the combination of neratinib and paclitaxel was 41.29%. Furthermore, at the doses tested, no death or apparent decrease in body weight was observed in the combination treatment groups, which suggests that the combination regimen did not increase the incidence of toxic side effects (Fig. 1C).

Neratinib Enhances the Intracellular Accumulation of Rho123 in Primary Leukemia Blasts with ABCB1 Overexpression and Sensitizes the Cells to ABCB1 Substrate Anticancer Drugs. Clinical samples of ABCB1-overexpressing leukemia cells from primary patients were used for ex vivo assessment of drug sensitization by neratinib. Primary leukemia blast samples exhibited ABCB1 on more than 10% of cells and were considered positive (Fig. 2A). We then examined the effect of neratinib on intracellular Rho123 accumulation in these ABCB1-overexpressing primary leukemia blasts with flow cytometric analysis. Our data showed that neratinib increased the levels of intracellular accumulation of Rho123 in a dose-dependent manner (0.25–1.0 μM). As shown in Fig. 2B, neratinib at 0.25, 0.5, and 1.0 μM increased intracellular Rho123 accumulation 1.26-, 1.40-, and 1.45-fold in cells from patient 1; 1.30-, 1.45-, and 1.69-fold in cells from patient 2; and 1.19-, 1.33-, and 1.77-fold in cells from patient 3, respectively. VRP (10 μM), a known ABCB1 inhibitor, also significantly enhanced Rho123 accumulation in all primary leukemia blasts.

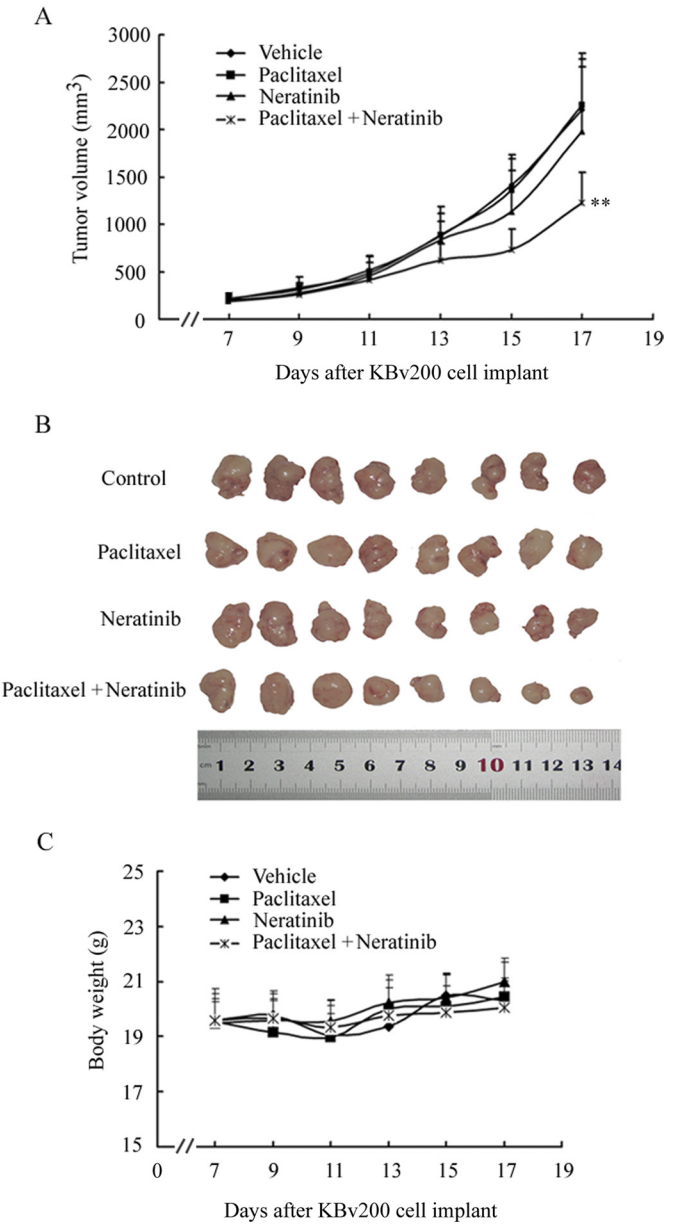

Fig. 1. Potentiation of the antitumor effects of paclitaxel by neratinib in a KBv200 xenograft model. KBv200 cells were collected and implanted into the mice for the chemotherapeutic studies. After 6 days, when the subcutaneous tumors were approximately 0.5 × 0.5 cm^2 (perpendicular diameters) in size, mice were divided randomly into the following four treatment groups: control (vehicle alone), neratinib (20 mg/kg p.o., every 3 days × four), paclitaxel (18 mg/kg i.p., every 3 days × four), and paclitaxel (18 mg/kg i.p., every 3 days × four) plus neratinib (20 mg/kg p.o., every 3 days × four, administered 1 h before paclitaxel administration). A, the tumor growth curve was drawn according to tumor volume and time of implantation. B, tumor tissues were excised from the mice and their weights were measured. C, animals' body weights were measured every 2 days, for modulation of the drug dosage. The mice were anesthetized and killed when the mean tumor weight in the control group was ~1 g. **, $P < 0.01$.

To demonstrate the sensitization effect of neratinib in the ex vivo model of ABCB1-overexpressing primary leukemia blasts, MTT cytotoxicity assays were performed. As shown in Fig. 2C, neratinib at 1.0 μM significantly sensitized all three primary leukemia blast samples to DOX treatment, com-

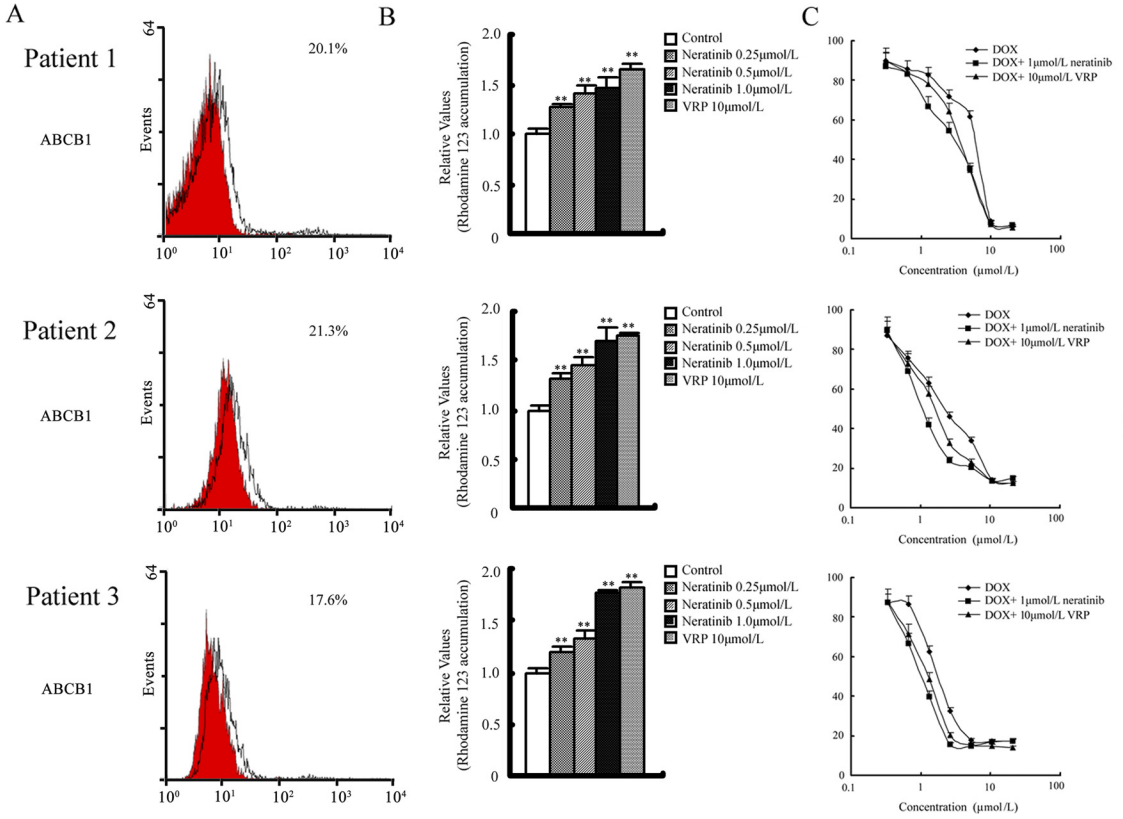

Fig. 2. Neratinib effects to increase the intracellular accumulation of Rho123 and to enhance the cytotoxicity of DOX in primary leukemia blasts with ABCB1 overexpression. Bone marrow samples were collected from three patients with newly diagnosed disease. A, expression of ABCB1 in primary leukemia blasts, determined through flow cytometry. Red and black histograms represent the isotype control and ABCB1, respectively. The proportions of ABCB1-positive cells are shown. B, intracellular accumulation of Rho123 in primary leukemia blasts with or without neratinib treatment, determined through flow cytometry. The relative levels of intracellular accumulation of Rho123 (in mean fluorescence intensity units), as determined through flow cytometry, were plotted. C, neratinib enhancement of DOX cytotoxicity in primary leukemia blasts with ABCB1 overexpression. Cytotoxicity was determined with MTT assays, as described under *Materials and Methods*. All data represent mean ± S.D. from at least three independent experiments performed in triplicate. **, $P < 0.01$.

pared with the control ($P < 0.05$). The IC_{50} values for DOX in the three primary leukemia blast samples were 1.49 ± 0.15, 1.94 ± 0.21, and 4.70 ± 0.45 μM and the reversal values were 2.62-, 1.96-, and 1.92-fold, respectively, at the concentration of 1.0 μM. The sensitization effect of neratinib at 1.0 μM was found to be similar to that of VRP at 10 μM. These results suggest that neratinib may be useful in sensitizing leukemia cells in patients to conventional anticancer agents and could be used to circumvent MDR in ABCB1-overexpressing leukemia cells. The relative efficacies of third-generation ABCB1-specific sensitizers such as tariquidar and zosuquidar are currently under clinical study and cannot be clearly compared with that of neratinib, because the levels of tumor growth inhibition in other nude mouse xenograft models were not calculated (Dantzig et al., 1996; Mistry et al., 2001); in vitro, zosuquidar reversed resistance to DOX in MCF-7/Adr cells 18- and 14-fold at 0.1 and 0.5 μM, respectively, which was similar to neratinib results (Table 1).

Neratinib Enhances the Accumulation of DOX and Rho123 in MDR Cells Overexpressing ABCB1. The results described above indicated that neratinib could enhance the sensitivity of MDR cancer cells to certain antineoplastic agents that are ABCB1 substrates. To elucidate the underlying mechanisms, the intracellular accumulation of DOX and Rho123 in the presence or absence of neratinib was examined through flow cytometric analysis. Upon treatment with the fluorescent substrates alone, the intracellular fluorescence intensity of DOX was significantly higher in KB (4.67-fold) and MCF-7 (3.61-fold) cells, compared with KBv200 and MCF-7/Adr cells, whereas that of Rho123 was 22.22-fold higher in KB cells and 16.01-fold higher in MCF-7 cells, compared with KBv200 and MCF-7/Adr cells, respectively (Fig. 3, A and B, and Supplemental Fig. 2). When the cells were treated with neratinib, the fluorescence index of DOX was increased 2.10-, 3.18-, and 3.84-fold in KBv200 cells and 1.57-, 2.15-, and 2.79-fold in MCF-7/Adr cells in the presence of 0.25, 0.5, and 1.0 μM neratinib, respectively. Likewise, neratinib at 0.25, 0.5, and 1.0 μM increased intracellular Rho123 accumulation 1.50-, 3.47-, and 8.77-fold in KBv200 cells and 3.86-, 5.68-, and 8.19-fold in MCF-7/Adr cells, respectively (Fig. 3, A and B, and Supplemental Fig. 2). However, no significant change in the intracellular accumulation of DOX and Rho123 was observed in parental MCF-7 and KB cells with combination treatment with neratinib. Taken together, these results suggest that neratinib is able to modulate ABCB1-mediated transport in MDR cells.

Neratinib Stimulates the ATPase Activity of ABCB1 at Low Concentration and Inhibits It at High Concentration. The drug-efflux function of ABCB1 is linked to ATP hydrolysis, and ATP consumption reflects the ATPase activity. To assess the effect of neratinib on the ATPase activity of ABCB1, we measured ABCB1-mediated ATP hydrolysis with

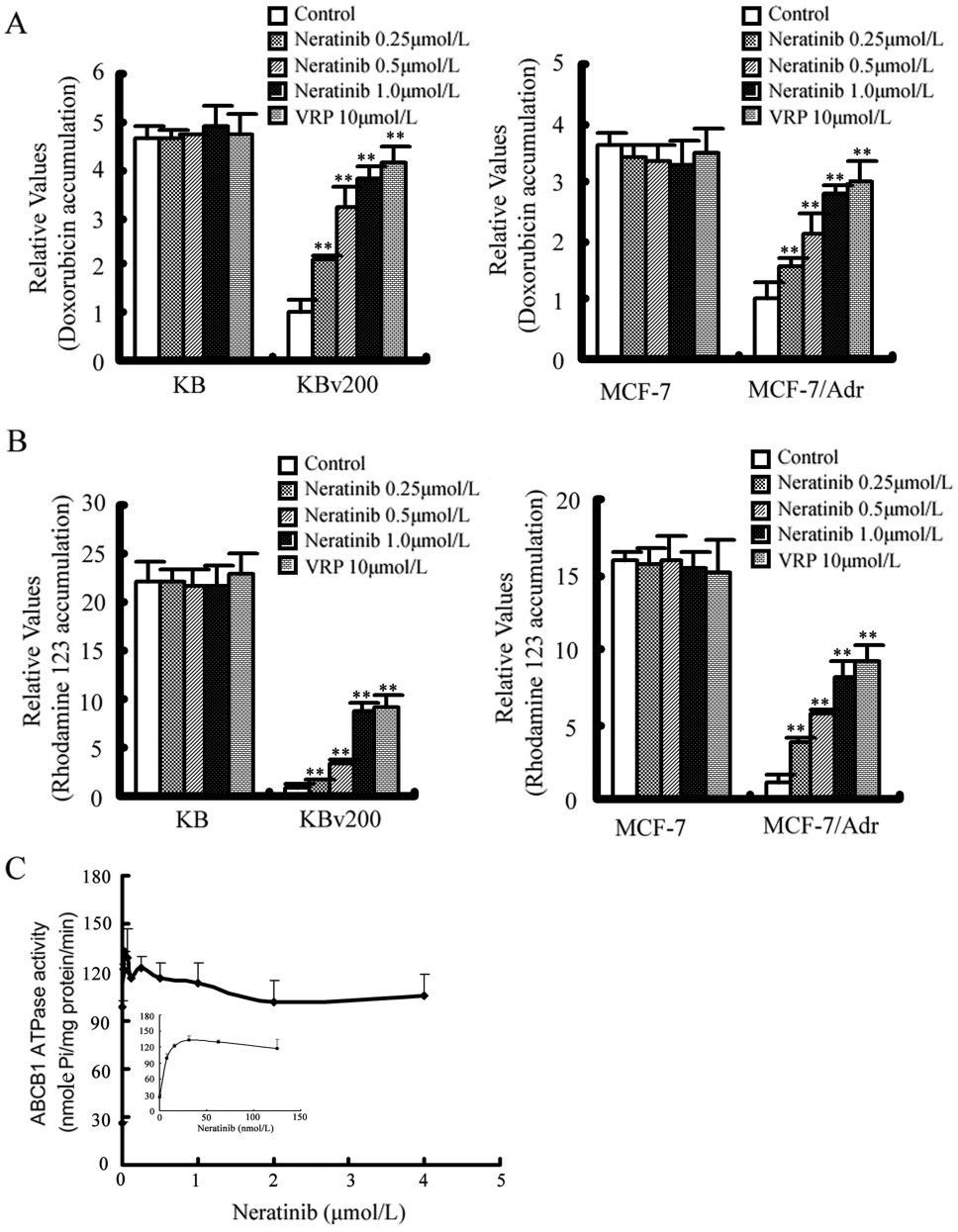

Fig. 3. Effects of neratinib on the accumulation of DOX and Rho123 and the activity of ABCB1 ATPase. A and B, accumulation of DOX (A) and Rho123 (B) measured through flow cytometric analysis, as described under *Materials and Methods*. The results are presented as fold changes in fluorescence intensity, relative to control MDR cells. Values were calculated by dividing the fluorescence intensity of each sample by that of MDR cells treated with DOX or Rho123 alone. Columns, means of triplicate determinations; bars, SD. **, $P < 0.01$, versus the MDR control group. C, luminescent ABCB1 ATPase assays performed according to Pgp-Glo assay system instructions. Inset, effects of lower concentrations of neratinib on ABCB1 ATPase. Each point represents the mean ± S.D. for three independent determinations.

various concentrations of neratinib. As shown in Fig. 3C, neratinib increased verapamil-stimulated ATPase activity at low concentrations and inhibited it at high concentrations.

Neratib Inhibits the Photoaffinity Labeling of ABCB1 with [^{125}I]IAAP. To determine whether neratinib interacts at the drug binding pocket of ABCB1, we tested its effect on the photolabeling of ABCB1 with an azido-[^{125}I]iodo-labeled transport substrate. As shown in Fig. 4, neratinib inhibited the photoaffinity labeling of ABCB1 with [^{125}I]IAAP in a concentration-dependent manner (IC_{50} = 0.24 ± 0.2 μM, n = 3), which indicates that neratinib interacts directly at the drug binding pocket of ABCB1.

Neratinib Does Not Alter the Expression of ABCB1 at the mRNA or Protein Level. The reversal of ABC transporter-mediated MDR can usually be achieved by decreasing transporter expression and/or inhibiting function. Therefore, we determined the effects of neratinib on the expression of ABCB1 at the mRNA and protein expression levels through reverse transcription-PCR, real-time RT-PCR, and Western blot analyses. Our results showed neither remarkable differences in ABCB1 expression at the protein and mRNA levels nor the intracellular location of the ABCB1 protein (Fig. 5, A–C, and Supplemental Figs. 3–5). These results indicate that down-regulation of the expression of ABCB1 is not involved in the reversal of ABCB1-mediated MDR by neratinib.

Neratinib Has No Effect on the Blockade of Akt Phosphorylation. The phosphorylation of Akt, which is the downstream marker of neratinib targeting, is usually used to test the targeted activity of neratinib. Previous studies showed that inhibition of the Akt pathway may enhance the efficacy of chemotherapeutic agents in cancer cells (Oh et al., 2006; Gagnon et al., 2008). To determine whether the reversal activity of neratinib is related to changes in the phosphorylation of Akt, we examined the phosphorylation of Akt with varying concentrations of neratinib. Lapatinib was used as a positive control to block the phosphorylation of Akt. As

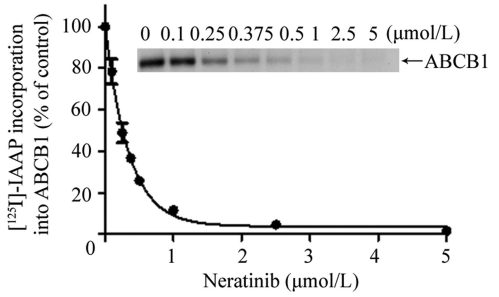

Fig. 4. Effect of neratinib on the photoaffinity labeling of ABCB1 with [^{125}I]IAAP. ABCB1-containing insect cell crude membranes (500 μg of protein/ml) were incubated with neratinib for 3 min at room temperature in 50 mM Tris-HCl, pH 7.5, after which 4 to 6 nM [^{125}I]IAAP was added. The samples were then exposed to UV light (365 nm) for 10 min at room temperature. The samples were resolved on 7% Tris-acetate gels, and the radioactivity incorporated into ABCB1 bands was determined by exposing the gels to X-ray film at −80°C and quantifying results by using a molecular imaging system and ImageQuaNT software (Sauna and Ambudkar, 2000). Top, autoradiogram from a representative experiment, showing the photoaffinity labeling of ABCB1 with [^{125}I]IAAP in the presence of neratinib at concentrations ranging from 0 to 5 μM. Bottom, IAAP incorporation data from ImageQuaNT analyses plotted with Prism 5 (GraphPad Software Inc., San Diego, CA). The values represent mean ± S.D. from three independent experiments.

shown in Fig. 5D, after exposure to 0.25, 0.5, 1.0, or 2.0 μM neratinib for 24 h or 1.0 μM neratinib for 3, 6, 12, or 24 h, the phosphorylation of Akt was not significantly changed. This suggests that the MDR reversal effect of neratinib in KBv200 cells is independent of the inhibition of Akt phosphorylation.

Neratinib Binding to ABCB1 Was Modeled. To understand the binding mechanism of neratinib in the homology model of human ABCB1 at the molecular level, we performed docking experiments by using all possible binding sites, as discussed above. Analysis of the binding energy data for the docked conformations of neratinib at each of binding sites 1 to 4 and the ATP binding site showed that neratinib binds most favorably at site 1 (Glide scores for neratinib binding at sites 1 to 4 and the ATP binding site were −11.23, −8.22, −7.29, −8.29, and −3.32 kcal/mol, respectively). Therefore, additional results and discussions are based on the binding interactions of neratinib at site 1.

The predicted binding conformation of neratinib within the large hydrophobic drug binding cavity (site 1) of human ABCB1 shows the importance of mainly hydrophobic and to some extent electrostatic interactions (Fig. 6A). For clarity, a schematic representation of neratinib interactions with site 1 residues is shown in Fig. 6B. The A-ring of neratinib is stabilized by hydrophobic contacts with the side chains of Phe728, Ala729, and Val982. The protonated tertiary amine function of the dimethylamino-but-2-enamide substitution present on the A-ring is involved in a cation-dipole type of interaction with the backbone carbonyl group of Ala985 (-R_3NH^+–O=C-Ala985; 3.6 Å). The carbonyl oxygen atom of the amide group present on the A-ring forms a hydrogen bond with the side-chain amide group of Gln725 (-CO–H_2NCO-Gln725; 2.2 Å), and the ether oxygen atom of the ethoxy group forms electrostatic interactions with the side chain of

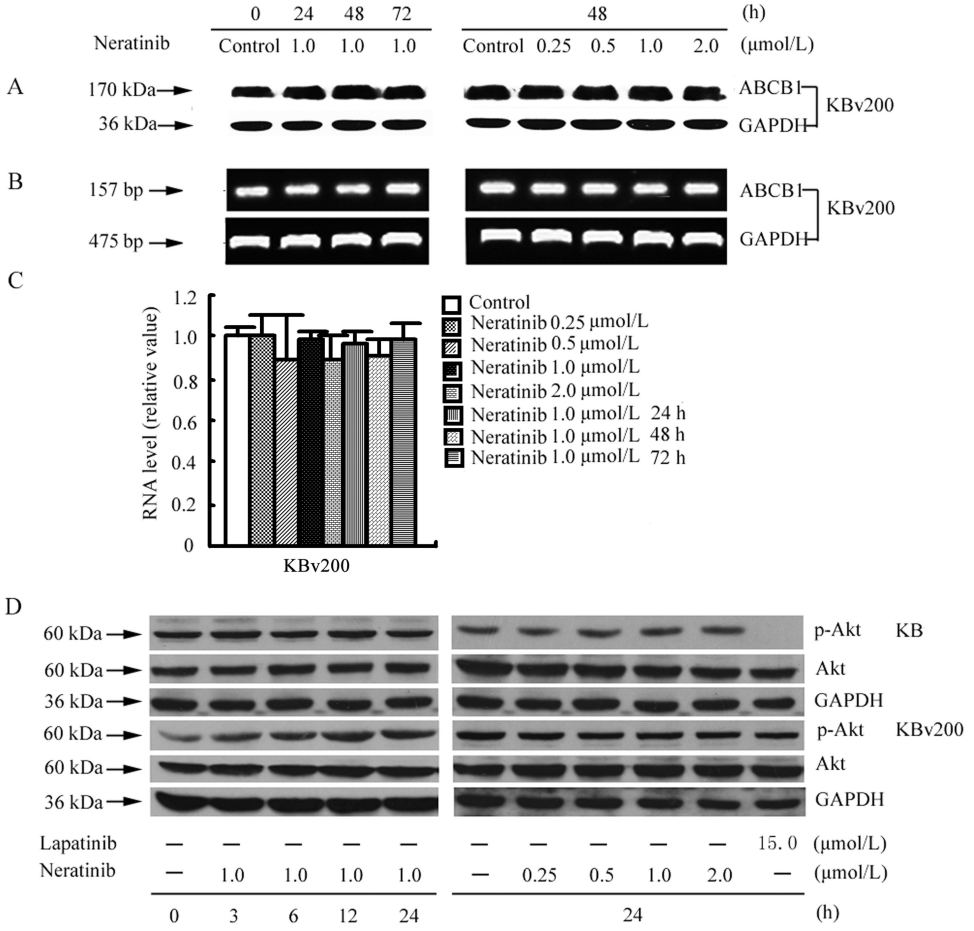

Fig. 5. Effects of neratinib on the expression of ABCB1 in MDR cells and the blockade of Akt phosphorylation. A, KBv200 cells were treated with neratinib at various concentrations for 48 h and at 1.0 μM for various times; equal amounts of total cell lysates were loaded and detected with Western blotting. B and C, mRNA levels for ABCB1 were determined with RT-PCR (B) and real-time PCR (C) assays, as described under *Materials and Methods*. A representative result from at least three independent experiments is shown. D, KB and KBv200 cells were treated with neratinib at various concentrations for 24 h and at 1.0 μM for various times. Equal amounts of protein were loaded for Western blot analysis, as described under *Materials and Methods*. Independent experiments were performed at least three times, and results from a representative experiment are shown. p-Akt, phosphorylated Akt.

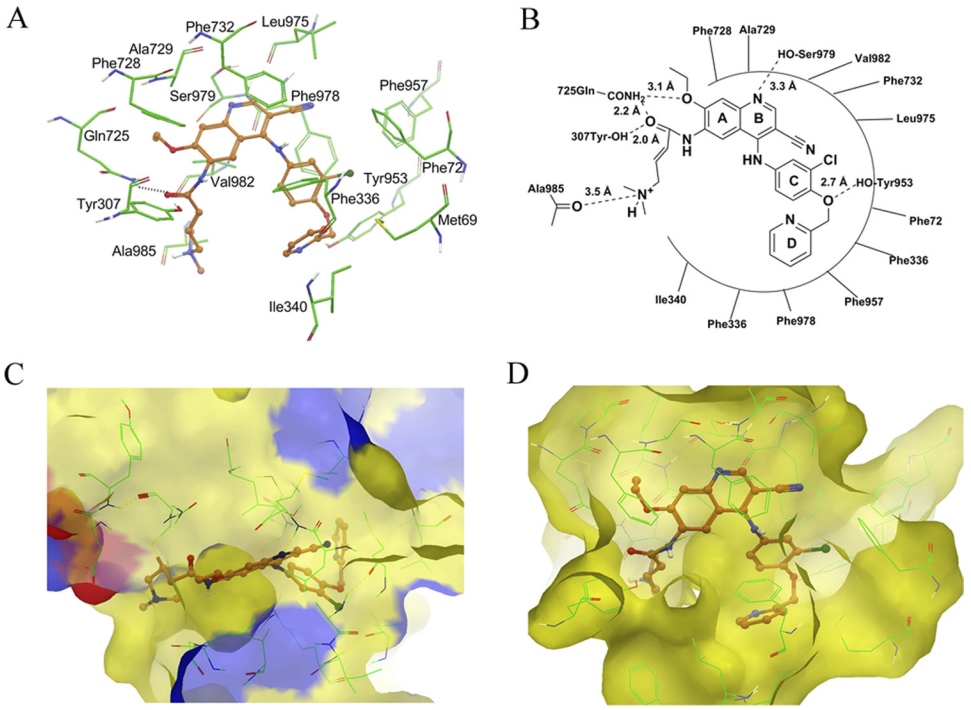

Fig. 6. Predicted binding conformation of neratinib within the large hydrophobic drug binding cavity (site 1) of human ABCB1, showing the importance of mainly hydrophobic and to some extent electrostatic interactions. The neratinib binding sites on the two targets share a significant hydrophobic component. A, XP-Glide–predicted binding conformation of neratinib within site 1 of human ABCB1. Important amino acids contacting neratinib are depicted as sticks, with the atoms colored as follows: carbon, green; hydrogen, white; nitrogen, blue; oxygen, red; sulfur, yellow. The inhibitor is shown as a ball-and-stick model with the same color scheme except that except carbon atoms are represented in orange and the chloro group in dark green. B, schematic representation of neratinib interactions with the site 1 residues of human ABCB1. C and D, EGFR (C) and human ABCB1 (D) represented as Macromodel surfaces according to residue charge [electropositive charge, blue; electronegative charge, red; neutral (hydrophobic), yellow], as implemented in Maestro. Covalently bound neratinib within the ATP binding site of EGFR and the docked conformation of neratinib within the drug binding cavity (site 1) of human ABCB1 are also shown, with the same color code as in A and B.

Gln725. The carbonyl oxygen atom of the amide group on the A-ring is also located within hydrogen-bonding distance from the hydroxyl function of Tyr307 (-CO–HO-Tyr307; 2.0 Å). Therefore, Gln725 and Tyr307 side chains seem to be conformationally locked through interaction with the amide group of the A-ring. The electron-deficient B-ring, which possesses a ring nitrogen atom and -CN substituent, is involved in face-to-face arene-arene interaction with the side chain of Phe732 and hydrophobic interaction with the side chain of Leu975. The B-ring nitrogen atom is located at an interacting distance (3.3 Å) from the side-chain hydroxyl group of Ser979. The hydrophobic residues Phe72, Phe336, Phe957, and Phe978 stabilize the C-ring of neratinib, and the D-ring is involved in hydrophobic interactions with the side chains of Met69, Phe336, and Ile340. The ether oxygen atom between the C-ring and the D-ring may enter into hydrogen bonding interactions with the side-chain hydroxyl group of Tyr953 (R_2O–HO-Tyr953; 2.7 Å).

Discussion

EGFR and Her-2 belong to the ErbB family of receptor tyrosine kinases, which are often overexpressed, dysregulated, or mutated in cancers (Rabindran et al., 2004). Agents targeting EGFR and/or Her-2 have shown encouraging therapeutic efficacy; such agents include trastuzumab, erlotinib (Cohen et al., 2005), and gefinitib (Cohen et al., 2003). Neratinib is an orally available small molecule that irreversibly inhibits EGFR and Her-2 by binding to their ATP binding sites (Rabindran et al., 2004). In the present study, our data showed for the first time that neratinib significantly potentiated the cytotoxicity of ABCB1 substrates in ABCB1-overexpressing cells. Furthermore, neratinib did not significantly change the sensitivity of ABCC1- and ABCG2-overexpressing cells to the substrates DOX and mitoxantrone, respectively (Table 1). These data suggested that the reversal ability of neratinib was quite specific to ABCB1.

In phase I and II trials, the maximal tolerated doses of neratinib for patients with solid tumors were 320 and 240 mg, respectively (Wong et al., 2009; Burstein et al., 2010; Sequist et al., 2010). The respective mean maximal concentrations were 119 and 73.5 ng/ml, equal to 0.214 and 0.132 μM. In vitro, the proportions of binding were similar (53–57%), and the covalent binding of neratinib to serum albumin was pH-, time-, and temperature-dependent but not substrate concentration-dependent, especially in the therapeutic range (Chandrasekaran et al., 2010). The concentrations of neratinib used in our experiments were 0.25, 0.5 and 1 μM, which were a little higher than the maximal concentrations in patients. However, higher concentrations may be detected in tumor tissues than in normal tissues and plasma, because of various functions of impaired tumor vasculature (Dreher et al., 2006). Therefore, the in vitro concentrations of neratinib used in our assays might be achieved in tumor tissues during therapeutic treatment.

In vivo, similar inhibitory effects of neratinib were demonstrated in multiple human tumor xenograft models, including 3T3/neu, A431, SK-OV-3, BT474, and MCF-7 cells (Rabindran et al., 2004). On the basis of those considerations, we chose neratinib (20 mg/kg) to determine its in vivo inhibition of tumor growth. We showed that the combination of paclitaxel with neratinib remarkably enhanced the anticancer activity of paclitaxel in the KBv200 xenograft model ($P < 0.05$) (Fig. 1, A and B).

It is noteworthy that in an ex vivo model of ABCB1-overexpressing primary leukemia blast cells obtained from three patients with newly diagnosed acute myeloid leukemia, neratinib could increase the accumulation of Rho123 (Fig. 2B) and enhance the cytotoxicity of DOX (Fig. 2C), which suggested that neratinib might be useful in circumventing MDR

in ABCB1-overexpressing leukemia cells. Consistent with the in vitro cytotoxic results, neratinib significantly enhanced the intracellular accumulation of DOX and Rho123 in ABCB1-overexpressing cells (Fig. 3, A and B, and Supplemental Fig. 2).

The profile of ATPase activity is considered to reflect the nature of interactions between the ABC transporters and the substrates. On the basis of their effects on ATPase activity, compounds could be categorized into three distinct types. Type I agents stimulate ATPase activity at low concentrations but inhibit activity at high concentrations (Mi et al., 2010). Type II compounds enhance ATPase activity in a dose-dependent manner, without any inhibition (Mi and Lou, 2007; Shi et al., 2007; Dai et al., 2008). Type III compounds inhibit both basal and verapamil-stimulated ATPase activity (Ambudkar et al., 1999; Tao et al., 2009). Neratinib should be classified as a type I modulator and may be a substrate of ABCB1 (Fig. 3C). Neratinib consistently inhibited photolabeling of ABCB1 with its substrate [^{125}I]IAAP, in a concentration-dependent manner (Fig. 4). The ATPase and IAAP data together demonstrate that, similar to other TKIs, neratinib directly interacts with ABCB1 at the drug binding pocket.

The expression of ABCB1 was not attenuated (Fig. 5, A–C, and Supplemental Figs. 3–5). It was reported that activation of the PI3K/Akt pathway is related to resistance to conventional anticancer drugs (Knuefermann et al., 2003). We found that neratinib (up to 2.0 μM) did not block the phosphorylation of Akt (Fig. 5D), which suggests that blockade of Akt activation is not involved in the reversal of ABCB1-mediated MDR by neratinib. Here we proposed that the MDR-reversal effect of neratinib is attributable to inhibition of the efflux function of ABCB1.

Furthermore, the most-negative binding energy of neratinib within the drug binding cavity (site 1) of human ABCB1 clearly indicated the drug binding cavity (site 1) as the most favorable site where binding of neratinib occurs. Because no attempts were made to rationalize such dual actions of TKIs, we sought to understand the cross-reactivity of TKIs with ABC transporters, particularly ABCB1. Because most of the TKIs, including neratinib, are hydrophobic in nature [the ClogP value generated for neratinib with QikProp 3.0 (Schrödinger, Inc.) is 4.45] and the ABCB1 transporter is rightly named a "hydrophobic vacuum cleaner," it is not surprising that TKIs are recognized at the hydrophobic drug binding cavity of the human ABCB1 transporter. Figure 6, C and D, clearly indicates that the neratinib binding sites on the two targets share a significant hydrophobic component, which provides computational support for the cross-reactivity of TKIs with the human ABCB1. Moreover, neratinib seems to exhibit all of the pharmacophoric features, such as hydrophobic groups and/or aromatic ring centers (A–D-rings), a hydrogen bond acceptor (amide group on the A-ring), and a positively charged ionizable group (tertiary amine), that are essential and reported for potent inhibitors of ABCB1. We hypothesize that the selectivity of neratinib for ABCB1 over ABCC1 and ABCG2 may be attributable to the fact that ABCB1 preferentially extrudes large hydrophobic drugs, whereas ABCC1 and ABCG2 transport relatively less-hydrophobic drugs that possess anionic groups. Although docking results have not been verified through site-directed mutagenesis or analysis of a neratinib-ABCB1 cocrystal complex, the neratinib docking model should form the basis for future lead compound optimization studies.

In general, the "first-generation" P-gp inhibitors, including verapamil, quinine, and cyclosporine, were ineffective or toxic at the doses required to attenuate P-gp function in vivo (Szakács et al., 2006). Second-generation agents (e.g., valspodar and biricodar) had better tolerability but were limited by unpredictable pharmacokinetic interactions with anticancer drugs (Rowinsky et al., 1998; Gottesman et al., 2002). Third-generation inhibitors (e.g., tariquidar, zosuquidar, and laniquidar) have high potency and specificity for P-gp. Furthermore, pharmacokinetic studies to date have shown that the third-generation inhibitors have no appreciable impact on CYP3A4 drug metabolism and no clinically significant drug interactions with commonly used chemotherapy agents (Patil et al., 2009). The relative efficacy of the third-generation ABCB1-specific sensitizers, such as tariquidar and zosuquidar, which are currently undergoing clinical trials, cannot be clearly compared with that of neratinib. The levels of tumor growth inhibition in other nude mouse xenograft models were not definitely calculated (Dantzig et al., 1996; Mistry et al., 2001), which makes it difficult to compare the in vivo inhibitory effects of the third-generation ABCB1-specific sensitizers with that of neratinib; however, in vitro zosuquidar reversed resistance to DOX 18- and 14-fold in MCF-7/Adr cells at 0.1 and 0.5 μM, respectively, findings that were similar to neratinib effects (Table 1).

Preclinical data suggested that neratinib was a substrate of CYP3A and was susceptible to interactions with potent CYP3A inhibitors and substrates. Therefore, dose adjustments may be necessary if neratinib is administered with such compounds (Abbas et al., 2011). Preliminary analyses of the trial results showed that neratinib could achieve stable disease control for more than 6 months in some patients with non–small-cell lung cancer that had progressed after treatment with gefitinib or erlotinib (Wong, 2007). Neratinib was evaluated in a phase II clinical trial with patients with advanced non–small-cell lung cancer who had previously received up to three chemotherapy regimens. Unfortunately, neratinib had low activity among patients with previous benefits from TKIs and TKI-naive patients, possibly because of insufficient bioavailability resulting from diarrhea-imposed dose limitations (Sequist et al., 2010).

Strategies to develop ABC transporter modulators as a therapeutic target to overcome drug resistance have failed in clinical settings to date (Shi et al., 2011). However, much effort is still being put into the development of ABC transporter modulators, as well as understanding the mechanism of action of ABC transporters. There is increasing evidence that ABC transporters are important in regulating oral bioavailability, pharmacological characteristics, and sanctuary site protection. Neratinib may have the potential to improve the chemotherapeutic outcomes for cancer patients through possibly several mechanisms of action (Shi et al., 2011).

In conclusion, our study showed that neratinib inhibited ABCB1-mediated drug efflux, which resulted in elevated intracellular concentrations of antineoplastic agents and increased drug sensitivity. Validation of MDR reversal by neratinib in a tumor xenograft model and leukemia blasts supports the potential effectiveness of combining neratinib with conventional anticancer drugs in surmounting clinical resistance in cancer chemotherapy.

Acknowledgments

We thank Dr. S. E. Bates (National Cancer Institute, National Institutes of Health) for MCF-7/FLV1000, HEK293/pcDNA3.1, and HEK293/ABCB1 cell lines.

Authorship Contributions

Participated in research design: Z.-S. Chen and Fu.
Conducted experiments: Zhao, Xie, X. Chen, Sim, and Liang.
Contributed new reagents or analytic tools: Singh and Talele.
Performed data analysis: Zhao, Sun, and Ambudkar.
Wrote or contributed to the writing of the manuscript: Zhao, Zhang, Talele, Ambudkar, Z.-S. Chen, and Fu.

References

Abbas R, Hug BA, Leister C, Burns J, and Sonnichsen D (2011) Pharmacokinetics of oral neratinib during co-administration of ketoconazole in healthy subjects. *Br J Clin Pharmacol* **71:**522–527.
Aller SG, Yu J, Ward A, Weng Y, Chittaboina S, Zhuo R, Harrell PM, Trinh YT, Zhang Q, Urbatsch IL, et al. (2009) Structure of P-glycoprotein reveals a molecular basis for poly-specific drug binding. *Science* **323:**1718–1722.
Alvarez RH (2010) Present and future evolution of advanced breast cancer therapy. *Breast Cancer Res* **12 (Suppl 2):**S1.
Ambudkar SV, Dey S, Hrycyna CA, Ramachandra M, Pastan I, and Gottesman MM (1999) Biochemical, cellular, and pharmacological aspects of the multidrug transporter. *Annu Rev Pharmacol Toxicol* **39:**361–398.
Bradford MM (1976) A rapid and sensitive method for the quantitation of microgram quantities of protein utilizing the principle of protein-dye binding. *Anal Biochem* **72:**248–254.
Burstein HJ, Sun Y, Dirix LY, Jiang Z, Paridaens R, Tan AR, Awada A, Ranade A, Jiao S, Schwartz G, et al. (2010) Neratinib, an irreversible ErbB receptor tyrosine kinase inhibitor, in patients with advanced ErbB2-positive breast cancer. *J Clin Oncol* **28:**1301–1307.
Chandrasekaran A, Shen L, Lockhead S, Oganesian A, Wang J, and Scatina J (2010) Reversible covalent binding of neratinib to human serum albumin in vitro. *Drug Metab Lett* **4:**220–227.
Chen LM, Liang YJ, Ruan JW, Ding Y, Wang XW, Shi Z, Gu LQ, Yang XP, and Fu LW (2004a) Reversal of P-gp mediated multidrug resistance in-vitro and in-vivo by FG020318. *J Pharm Pharmacol* **56:**1061–1066.
Chen LM, Wu XP, Ruan JW, Liang YJ, Ding Y, Shi Z, Wang XW, Gu LQ, and Fu LW (2004b) Screening novel, potent multidrug-resistant modulators from imidazole derivatives. *Oncol Res* **14:**355–362.
Cohen MH, Johnson JR, Chen YF, Sridhara R, and Pazdur R (2005) FDA drug approval summary: erlotinib (Tarceva) tablets. *Oncologist* **10:**461–466.
Cohen MH, Williams GA, Sridhara R, Chen G, and Pazdur R (2003) FDA drug approval summary: gefitinib (ZD1839) (Iressa) tablets. *Oncologist* **8:**303–306.
Dai CL, Liang YJ, Wang YS, Tiwari AK, Yan YY, Wang F, Chen ZS, Tong XZ, and Fu LW (2009) Sensitization of ABCG2-overexpressing cells to conventional chemotherapeutic agent by sunitinib was associated with inhibiting the function of ABCG2. *Cancer Lett* **279:**74–83.
Dai CL, Tiwari AK, Wu CP, Su XD, Wang SR, Liu DG, Ashby CR Jr, Huang Y, Robey RW, Liang YJ, et al. (2008) Lapatinib (Tykerb, GW572016) reverses multidrug resistance in cancer cells by inhibiting the activity of ATP-binding cassette subfamily B member 1 and G member 2. *Cancer Res* **68:**7905–7914.
Dantzig AH, Shepard RL, Cao J, Law KL, Ehlhardt WJ, Baughman TM, Bumol TF, and Starling JJ (1996) Reversal of P-glycoprotein-mediated multidrug resistance by a potent cyclopropyldibenzosuberane modulator, LY335979. *Cancer Res* **56:**4171–4179.
Dean M, Rzhetsky A, and Allikmets R (2001) The human ATP-binding cassette (ABC) transporter superfamily. *Genome Res* **11:**1156–1166.
Dreher MR, Liu W, Michelich CR, Dewhirst MW, Yuan F, and Chilkoti A (2006) Tumor vascular permeability, accumulation, and penetration of macromolecular drug carriers. *J Natl Cancer Inst* **98:**335–344.
Fu L, Liang Y, Deng L, Ding Y, Chen L, Ye Y, Yang X, and Pan Q (2004) Characterization of tetrandrine, a potent inhibitor of P-glycoprotein-mediated multidrug resistance. *Cancer Chemother Pharmacol* **53:**349–356.
Gagnon V, Van Themsche C, Turner S, Leblanc V, and Asselin E (2008) Akt and XIAP regulate the sensitivity of human uterine cancer cells to cisplatin, doxorubicin and taxol. *Apoptosis* **13:**259–271.
Gottesman MM, Fojo T, and Bates SE (2002) Multidrug resistance in cancer: role of ATP-dependent transporters. *Nat Rev Cancer* **2:**48–58.
Knuefermann C, Lu Y, Liu B, Jin W, Liang K, Wu L, Schmidt M, Mills GB, Mendelsohn J, and Fan Z (2003) HER2/PI-3K/Akt activation leads to a multidrug resistance in human breast adenocarcinoma cells. *Oncogene* **22:**3205–3212.
Livak KJ and Schmittgen TD (2001) Analysis of relative gene expression data using real-time quantitative PCR and the $2(-\Delta\Delta C_T)$ method. *Methods* **25:**402–408.
Mi Y and Lou L (2007) ZD6474 reverses multidrug resistance by directly inhibiting the function of P-glycoprotein. *Br J Cancer* **97:**934–940.
Mi YJ, Liang YJ, Huang HB, Zhao HY, Wu CP, Wang F, Tao LY, Zhang CZ, Dai CL, Tiwari AK, et al. (2010) Apatinib (YN968D1) reverses multidrug resistance by inhibiting the efflux function of multiple ATP-binding cassette transporters. *Cancer Res* **70:**7981–7991.
Mistry P, Stewart AJ, Dangerfield W, Okiji S, Liddle C, Bootle D, Plumb JA, Templeton D, and Charlton P (2001) In vitro and in vivo reversal of P-glycoprotein-mediated multidrug resistance by a novel potent modulator, XR9576. *Cancer Res* **61:**749–758.
Oh SY, Song JH, Gil JE, Kim JH, Yeom YI, and Moon EY (2006) ERK activation by thymosin-beta-4 (TB4) overexpression induces paclitaxel-resistance. *Exp Cell Res* **312:**1651–1657.
Patil Y, Sadhukha T, Ma L, and Panyam J (2009) Nanoparticle-mediated simultaneous and targeted delivery of paclitaxel and tariquidar overcomes tumor drug resistance. *J Control Release* **136:**21–29.
Pérez-Tomás R (2006) Multidrug resistance: retrospect and prospects in anti-cancer drug treatment. *Curr Med Chem* **13:**1859–1876.
Rabindran SK, Discafani CM, Rosfjord EC, Baxter M, Floyd MB, Golas J, Hallett WA, Johnson BD, Nilakantan R, Overbeek E, et al. (2004) Antitumor activity of HKI-272, an orally active, irreversible inhibitor of the HER-2 tyrosine kinase. *Cancer Res* **64:**3958–3965.
Robey RW, Honjo Y, Morisaki K, Nadjem TA, Runge S, Risbood M, Poruchynsky MS, and Bates SE (2003) Mutations at amino-acid 482 in the *ABCG2* gene affect substrate and antagonist specificity. *Br J Cancer* **89:**1971–1978.
Robey RW, Medina-Pérez WY, Nishiyama K, Lahusen T, Miyake K, Litman T, Senderowicz AM, Ross DD, and Bates SE (2001) Overexpression of the ATP-binding cassette half-transporter, ABCG2 (Mxr/BCrp/ABCP1), in flavopiridol-resistant human breast cancer cells. *Clin Cancer Res* **7:**145–152.
Rowinsky EK, Smith L, Wang YM, Chaturvedi P, Villalona M, Campbell E, Aylesworth C, Eckhardt SG, Hammond L, Kraynak M, et al. (1998) Phase I and pharmacokinetic study of paclitaxel in combination with biricodar, a novel agent that reverses multidrug resistance conferred by overexpression of both MDR1 and MRP. *J Clin Oncol* **16:**2964–2976.
Sauna ZE and Ambudkar SV (2000) Evidence for a requirement for ATP hydrolysis at two distinct steps during a single turnover of the catalytic cycle of human P-glycoprotein. *Proc Natl Acad Sci USA* **97:**2515–2520.
Sequist LV, Besse B, Lynch TJ, Miller VA, Wong KK, Gitlitz B, Eaton K, Zacharchuk C, Freyman A, Powell C, et al. (2010) Neratinib, an irreversible pan-ErbB receptor tyrosine kinase inhibitor: results of a phase II trial in patients with advanced non-small-cell lung cancer. *J Clin Oncol* **28:**3076–3083.
Seyhan AA, Varadarajan U, Choe S, Liu Y, McGraw J, Woods M, Murray S, Eckert A, Liu W, and Ryan TE (2011) A genome-wide RNAi screen identifies novel targets of neratinib sensitivity leading to neratinib and paclitaxel combination drug treatments. *Mol Biosyst* **7:**1974–1989.
Shi Z, Liang YJ, Chen ZS, Wang XW, Wang XH, Ding Y, Chen LM, Yang XP, and Fu LW (2006) Reversal of MDR1/P-glycoprotein-mediated multidrug resistance by vector-based RNA interference in vitro and in vivo. *Cancer Biol Ther* **5:**39–47.
Shi Z, Peng XX, Kim IW, Shukla S, Si QS, Robey RW, Bates SE, Shen T, Ashby CR Jr, Fu LW, et al. (2007) Erlotinib (Tarceva, OSI-774) antagonizes ATP-binding cassette subfamily B member 1 and ATP-binding cassette subfamily G member 2-mediated drug resistance. *Cancer Res* **67:**11012–11020.
Shi Z, Tiwari AK, Shukla S, Robey RW, Singh S, Kim IW, Bates SE, Peng X, Abraham I, Ambudkar SV, et al. (2011) Sildenafil reverses ABCB1- and ABCG2-mediated chemotherapeutic drug resistance. *Cancer Res* **71:**3029–3041.
Sissung TM, Gardner ER, Piekarz RL, Howden R, Chen X, Woo S, Franke R, Clark JA, Miller-DeGraff L, Steinberg SM, et al. (2011) Impact of ABCB1 allelic variants on QTc interval prolongation. *Clin Cancer Res* **17:**937–946.
Szakács G, Paterson JK, Ludwig JA, Booth-Genthe C, and Gottesman MM (2006) Targeting multidrug resistance in cancer. *Nat Rev Drug Discov* **5:**219–234.
Tao LY, Liang YJ, Wang F, Chen LM, Yan YY, Dai CL, and Fu LW (2009) Cediranib (recentin, AZD2171) reverses ABCB1- and ABCC1-mediated multidrug resistance by inhibition of their transport function. *Cancer Chemother Pharmacol* **64:**961–969.
Tsou HR, Overbeek-Klumpers EG, Hallett WA, Reich MF, Floyd MB, Johnson BD, Michalak RS, Nilakantan R, Discafani C, Golas J, et al. (2005) Optimization of 6,7-disubstituted-4-(arylamino)quinoline-3-carbonitriles as orally active, irreversible inhibitors of human epidermal growth factor receptor-2 kinase activity. *J Med Chem* **48:**1107–1131.
Wong KK (2007) HKI-272 in non small cell lung cancer. *Clin Cancer Res* **13:**s4593–s4596.
Wong KK, Fracasso PM, Bukowski RM, Lynch TJ, Munster PN, Shapiro GI, Jänne PA, Eder JP, Naughton MJ, Ellis MJ, et al. (2009) A phase I study with neratinib (HKI-272), an irreversible pan ErbB receptor tyrosine kinase inhibitor, in patients with solid tumors. *Clin Cancer Res* **15:**2552–2558.
Yan Y, Su X, Liang Y, Zhang J, Shi C, Lu Y, Gu L, and Fu L (2008) Emodin azide methyl anthraquinone derivative triggers mitochondrial-dependent cell apoptosis involving in caspase-8-mediated Bid cleavage. *Mol Cancer Ther* **7:**1688–1697.
Yan YY, Zheng LS, Zhang X, Chen LK, Singh S, Wang F, Zhang JY, Liang YJ, Dai CL, Gu LQ, et al. (2011) Blockade of Her2/neu binding to Hsp90 by emodin azide methyl anthraquinone derivative induces proteasomal degradation of Her2/neu. *Mol Pharm* **8:**1687–1697.
Yun CH, Mengwasser KE, Toms AV, Woo MS, Greulich H, Wong KK, Meyerson M, and Eck MJ (2008) The T790M mutation in EGFR kinase causes drug resistance by increasing the affinity for ATP. *Proc Natl Acad Sci USA* **105:**2070–2075.
Zheng LS, Wang F, Li YH, Zhang X, Chen LM, Liang YJ, Dai CL, Yan YY, Tao LY, Mi YJ, et al. (2009) Vandetanib (Zactima, ZD6474) antagonizes ABCC1- and ABCG2-mediated multidrug resistance by inhibition of their transport function. *PLoS One* **4:**e5172.

Address correspondence to: Dr. Li-wu Fu, State Key Laboratory of Oncology in South China, Cancer Center, Sun Yat-Sen University, Guangzhou, 510060, China. E-mail: fulw@mail.sysu.edu.cn